Control of Adhesion and Surface Forces via Potential-Dependent Adsorption of Pyridine

Joëlle Fréchette and T. Kyle Vanderlick*

Department of Chemical Engineering, Princeton University, Princeton, New Jersey 08540

Received: October 5, 2004; In Final Form: December 11, 2004

The orientation and extent of adsorption of pyridine on a gold electrode is known to depend on applied potential and is well characterized. By use of the electrochemical surface forces apparatus, we measured the potential dependence of the double-layer interactions and adhesive forces between a gold electrode and a mica surface for different pyridine concentrations. We observed that, unlike mica−mica interactions, the gold−mica interactions were strongly affected by the presence of small concentrations of pyridine. We are able to reach high negative surface potentials (as determined by applying Derjaguin−Landau−Verway−Overbeek theory to our force measurements), which is similar to what is observed in the absence of pyridine. This demonstrates the electronic nature of the forces measured and shows that pyridine does not displace potential-determining ions on the surface. At positive potentials, where the interaction between gold and mica is attractive, pull-off measurements are a strong function of applied potential. The major effect of the presence of pyridine is on the observed shift in the potential of zero force (PZF), moving it to more negative potentials. This effect is caused by the strong dipole of the pyridine molecule. When the applied potential is cast as a deviation from the PZF, the effect of pyridine is to reduce adhesion between gold and mica. We modeled the potential-dependent adhesion of this system using an electrocapillary framework developed previously, and in doing so, we establish the relationship between the gold−liquid and gold−mica surface energies. In addition, we show that pyridine adsorption affects the capacitance of the gold−mica interface.

Introduction

The response of an electrode is very sensitive to its environment. Small changes in solution composition can have profound effects on the kinetics of electrochemical reactions. Adsorption at the electrode/electrolyte interface can inhibit or facilitate a reaction depending on the nature of the adsorbent and its interaction with the surface.[1−3] Some neutral organic molecules, such as pyridine, have unusual behaviors in which the extent of adsorption or the orientation of the adsorbed molecules vary with the electrode potential.[4]

A great deal of work has been done studying pyridine adsorption from aqueous solution on metal electrodes. Adsorption on group IB metals such as gold, copper, and silver is very different than adsorption on mercury or even platinum.[4] Pyridine adsorption on gold has been characterized as a weak chemisorption in which pyridine replaces water molecules on the gold surface.[5] Pyridine has a stronger dipole moment than water, so its adsorption causes a shift of the potential of zero charge (PZC) to more negative values. There is also some evidence of partial electron transfer between the gold surface and the pyridine molecule.[6] There is a change in the orientation of the aromatic ring in the pyridine molecule (from flat on the surface to vertical) as a function of applied potential on the gold surface.[6] At the PZC, the ring lays flat on the gold surface, while at more positive potentials, it flips and stands up with the nitrogen atom on the surface, thereby allowing increased surface concentration. The potential at which this reorientation occurs varies for the different crystallographic planes of gold; some facets show no pyridine reorientation (the ring stands up at all potentials).[5] Polycrystalline gold electrodes behave as a combination of all the crystal planes. The adsorption of pyridine is also reversible; it desorbs from the surface at high negative potentials, making the gold−pyridine system dynamic.[6] The nature and extent of pyridine adsorption has been well characterized using a wide variety of techniques from differential capacitance[7] to radiotracers,[8] spectroscopy,[9] and chronocoulometry.[6]

Investigating the impact of pyridine adsorption on surface forces offers a new perspective on active control of interfacial properties,[10] where external and reversible control of characteristics such as wetting, adhesion, and surface energy is used as the *active* component of a device. For example, pyridine could affect the potential dependence of surface forces, effectively acting as an additional controllable parameter for surface interactions. In addition, the way by which pyridine, a neutral highly polar molecule, can affect the interaction between an electrode and another surface is of fundamental interest. Intuitively, because of its neutrality, pyridine in solution should not affect the structure of the diffuse ionic double layer next to the electrode. Therefore, the decay length of the long-range double-layer forces should remain the same when pyridine is present. On the other hand, the presence of pyridine on the electrode surface should have an impact on interactions near contact such as short-range forces and adhesion.

Larson et al.[11] investigated the competition between pyridine and citrate ions on a gold surface by measuring time-dependent double-layer interactions. They observed a rapid disappearance of long-range double-layer interactions and an increase in hydration forces once pyridine is added in solution. Their work showed that pyridine displaces the citrate ions from the surface, leaving the gold surface uncharged along with revealing the importance of citrate adsorption in the stabilization of gold sols. Using an electrode instead of a metal surface as one of the interacting substrates transforms the system under study from

* Author to whom correspondence may be addressed. Phone: (609) 258-4891. Fax: (609) 258-0211. E-mail: vandertk@princeton.edu.

10.1021/jp0454669 CCC: $30.25
Published on Web 02/12/2005

static to dynamic (given the reversibility of pyridine adsorption with applied potential). In addition, part, if not all, of the charge on an electrode is electronic in nature, therefore the presence of pyridine can hardly "displace" the charge on the surface. The charge on the electrode can be affected, however, by image charges caused by the larger dipole moment of pyridine (compared to that of water).[12]

In this work, we describe measurements of double-layer interactions and adhesion between a gold electrode and a mica surface for different pyridine concentrations using the electrochemical surface forces apparatus (ESFA).[13] We investigated the effect of pyridine on mica−mica and gold−mica forces in a noninteracting potassium perchlorate background salt solution. We observed that pyridine did not alter mica−mica interactions over a range of pyridine concentrations but did have notable effects on gold−mica interactions. The most significant of these is a shift in the value of the potential of zero force (PZF) to more negative potentials as the concentration of pyridine is increased. We also demonstrate that the effect of pyridine on adhesion can be understood in terms of an electrocapillary approach we have previously developed.[14] This approach reveals the relationship between the gold−liquid and the gold−mica surface energies.

Experimental Section

ESFA. ESFA[13] is a modified version of the original SFA developed over 30 years ago[15,16] allowing potential control of one or both of the surfaces studied. The key modification is the substitution of uniquely fabricated electrodes for the mica substrates commonly used in the apparatus.[17] Briefly, electrodes for use in the ESFA are made by gluing a clean, molecularly smooth piece of mica to the standard silica disk employed in the SFA. The mica piece is then treated with oxygen plasma and masked by another, smaller, mica piece, which remains held by van der Waals forces. Next, an adhesive layer of titanium (ca. 15 nm) is evaporated on the mica followed immediately by a thick (ca. 150 nm) layer of gold. Pure indium is then used to solder a fine gold wire at the extreme corner of the gold-covered mica sheet, and a layer of epoxy subsequently covers the connection. Finally, the masking mica piece is removed, and final thin layers of titanium (ca 1.5 nm) and gold (ca. 60 nm) are evaporated creating a gold region at the center of the substrate, thin enough for effective employment of multiple beam interferometry. The electrode is used immediately in the SFA.

Beyond electrode preparation, having potential control inside the SFA requires additional considerations. We use a Teflon bath for the electrolyte instead of filling the whole chamber. The gold electrode described above is connected to a potentiostat (PAR 263A, Oak Ridge, TN) as a working electrode, and a gold gauze (82 mesh, 99.9%, Alfa, Ward Hill, MA) is placed inside the Teflon bath as a counterelectrode. The reference electrode is a palladium Ag_2S wire.[18] The potential of the gold electrode is translated to an Ag/AgCl (3 M) (Brinkmann, Westbury, NY) scale by measuring the open circuit potential difference between the two references at the end of each experiment. All potential values in this work are expressed with respect to the Ag/AgCl (3 M) reference electrode. Forces and adhesion measurements are performed within the double-layer potential window (i.e., where the gold electrode can be considered ideally polarized) as determined by cyclic voltammetry.

There are two major issues regarding the measurements of surface separation in the ESFA: the nature of the optical filter (titanium/gold/solution/mica/silver) and the roughness of the gold surface. The unsymmetrical nature of the optical filter prevents one from using simple analytical expressions based on the reference case of zero surface separation.[19] Instead, the multimatrix method[20,21] must be employed, and this requires that the thicknesses of the mica be explicitly known. The mica thickness is determined by interferometry using pieces of equivalent thickness to that used in the ESFA. The roughness of the gold surface is taken into account by modeling the rough gold substrate as two-layer system composed of a smooth gold substrate with a uniform dielectric overcoat of thickness on the order of the RMS of the gold (we have previously referred to this overcoat as a "residual dielectric gap").[22] The values we determined for the dielectric gap varied between 40 and 60 Å for each experiment. During force measurements, the separation is inferred from the increase in the dielectric thickness beyond that which accounts for the residual dielectric gap.

Materials. Solutions of 1 mM $KClO_4$ with pyridine (0.2−100 mM) were prepared from highest available purity solutes (99.99%, Aldrich, Miliwaukee, WI), which were used without further purification and dissolved in 18.2 MΩ deionized water (Hydro Services, Levittown, PA). The solutions were unbuffered and had a pH of about 5.5. The gold working electrode was made by thermal evaporation (ca. 2.0 Å/s) using high-purity gold (99.999%, Cerac, Miliwaukee, WI) and titanium (99.99%, Alfa). The roughness was characterized using atomic force microscopy (AFM) as having an RMS of 3 nm.[23,24] Solder was high-purity indium (99.999%, Cerac) and covered with epoxy (Hysol, 0151, Dexter, CA). Mica sheets (Ruby, ASTM V-2, S&J Trading, NY) were cleaved in a laminar hood and put on a larger mica backing sheet. This backing sheet was then coated with a silver (99.999%, Alfa) film approximately 48 nm thick (formed at a rate of 3.5 Å/s). Mica substrates for use in the ESFA were created by peeling a small mica sheet off the backing plate and gluing it silver side down onto a silica disk with a thermoset epoxy (Shell, Epon 1004).

Procedure. The cleaning procedure carried out before every experiment has been described previously.[13] Once the apparatus was completely assembled with all electrical connections in place, gold and mica were brought into contact in air, and the fringe positions were recorded. The surfaces were then separated, and the solution was injected using a reagent bottle pressurized with humid nitrogen and equipped with all Teflon tubing and valves (Omnifit, Rockville Center, NY). The solution was deaerated with humid nitrogen for 30 min before use, and the experiment was done under a slight positive pressure of nitrogen. The solution was left in the apparatus for 1−2 h for equilibration. The potential of the gold electrode was controlled with a potentiostat. Current was also monitored during the force measurements to ensure that there was little faradaic current. A charge-coupled device camera (Photometrics, Tucson, AZ) was used to determine the positions of interference fringes from which pull-off separations, as well as the mean radius of curvature of the interacting substrates, were calculated. The fringe positions yielding the separation dependence of the double-layer forces were recorded manually. For experiments involving two mica surfaces, the same procedure was followed without the use of electrodes. All experiments were performed at 22 °C in a controlled-temperature environment.

Results and Discussion

As a prelude to studying the impact of pyridine on gold−mica interactions, we investigated the effect of pyridine on

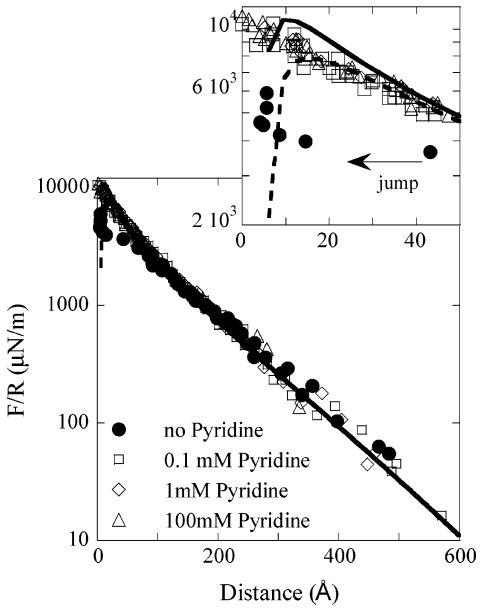

Figure 1. Measured forces (normalized with the radius of curvature) between two mica surfaces in 10^{-3} M $KClO_4$ and different pyridine concentrations. The inset shows forces at short separations. The lines correspond to the best fit for DLVO predictions for a Debye length of 9.6 nm and a surface potential at infinite separation of $\psi^{\infty} = -130$ mV. The upper line is for constant charge, and the lower dashed line is for constant potential.

mica−mica interactions. Figure 1 shows the double-layer interactions measured between two mica sheets in a background of 1 mM $KClO_4$ for different pyridine concentrations (0.2, 1, and 100 mM). $KClO_4$ was chosen because it is known not to have specific adsorption on gold.[25] The fitted lines correspond to a theoretical prediction using standard Derjaguin−Landau−Verway−Overbeek (DLVO) theory[26,27] calculated by solving numerically the nonlinear Poisson−Boltzmann equation (using a Hamaker constant of 2.2×10^{-20} J to represent the van der Waals forces[16]). The Debye length was not fitted; rather, it was calculated from the injected salt concentration. By use of DLVO theory, a surface potential of −130 mV was determined.

A unique characteristic of the SFA is its capability to measure independently the absolute surface separation (using interferometry) with a resolution of around ±2 Å. This is in contrast to the AFM where the surface separation is inferred from the forces measured (zero separation is associated with the onset of the constant compliance regime). By use of the SFA, the wavelengths of the fringes at contact are measured, and a variation in those wavelengths during an experiment is evidence of a change in the absolute separation of the two interacting surfaces (which can be caused by adsorption of hard films or molecular layers). For the mica−mica experiments, we see no evidence of contact fringes shifting to longer wavelengths due to pyridine adsorption on mica. More specifically, the contact fringes show no change within the resolution limit of the apparatus across all experiments (in terms of surface separation, our resolution is around ±2 Å). Pyridine with the ring lying flat on a surface has a height of around 3 Å and with the ring in the vertical position has a maximum height of 8 Å[28] (while a water molecule is roughly 3 Å). Previous surface-forces experiments have shown that the last layer of adsorbed water is often tightly bound to the surface and not necessarily removed when the surface is immersed solution.[29] Thus, it would be difficult to observe a change in contact if pyridine displaces water and binds to the surface in the flat orientation. However, if pyridine were bound at the surface with its ring standing up, our technique would have detected a measurable shift in wavelengths of the contact fringes (which we do not observe).

For interactions between mica surfaces (Figure 1), the presence of pyridine did not measurably affect the surface potential or the Debye length. Previous work examining the effect of 2% pyridine on the interaction between two silica surfaces showed that pyridine reduced significantly the Debye length, an effect assumed to be caused by the basic nature of the pyridine molecule.[30] This was not observed in our experiments, but the highest concentration we used was lower than the pyridine concentration employed in the silica−silica experiments (our highest concentration was 0.8% per volume while theirs was 2%). In addition, we used a 1 mM background salt, while their experiments were done in pure water.

At short-range (separations smaller than the Debye length), we see that surface forces are more repulsive in the presence of pyridine than when only the background salt is present, as seen in the inset of Figure 1. Forces do not reach the attractive minimum predicted by standard DLVO theory (which is readily observed in the background salt). Non-DLVO forces between mica surfaces are thought to be due to the extra work required to remove the hydration sheath of cations (i.e., the last layer of adsorbed water) on the mica surface (also called hydration or solvation forces).[31] A similar effect would be anticipated to remove a layer of surface-bound pyridine. Indeed, calculations have shown that pyridine binding may have a slight energetic advantage compared to water for mica surfaces,[32] in which case the non-DLVO forces would be greater in the presence of pyridine. The absence of the attractive minimum is not unique to addition of pyridine. Similar non-DLVO forces are often observed at salt concentrations higher than 1 mM and sometimes even at lower salt concentrations.[29,31,33] Increasing the pyridine concentration from 0.2 to 100 mM does not increase the extent of non-DLVO forces further; no dependence of hydration forces on pyridine concentration can be seen. Overall, pyridine has a minimal effect on mica−mica interactions: the Debye length remains unchanged, the surface potential remains constant, and the non-DLVO forces are weak.

Figure 2 shows repulsive double-layer forces between a mica surface and gold electrode for different applied potentials and for different pyridine concentrations. Three concentrations of pyridine were used (0.2, 1, and 100 mM) in a 1 mM $KClO_4$ background. As observed for mica−mica interactions, the presence of pyridine does not change the observed Debye length; all decay lengths correspond to the background 1 mM salt concentration. Some characteristics of the long-range double-layer forces are similar to those in the background salt only. Parts a−c of Figure 2 show the high negative surface potential obtained (from fitting the data to DLVO theory), effectively reaching the saturation limit (e.g., see the upper curve in Figure 2b). Also observable in Figure 2 is the small change in applied potential required to modify the double-layer forces from highly repulsive to attractive (e.g., see the rapid drop in surface potentials between the two lower curves in Figure 2b).

This similarity between parts a−c of Figure 2 highlights the electronic nature of the charge on the gold surface (i.e., externally applied by the potentiostat). If the large negative surface potentials reached on the gold surface in the background salt (Figure 2a) were, instead, caused by adsorption of negatively charged perchlorate ions, then adsorption of pyridine would displace those ions and high negative surface potentials would not be reached (since pyridine is a neutral molecule, there would be a drop in the charge on the electrode, which would cause lower surface potentials). This displacement effect was previ-

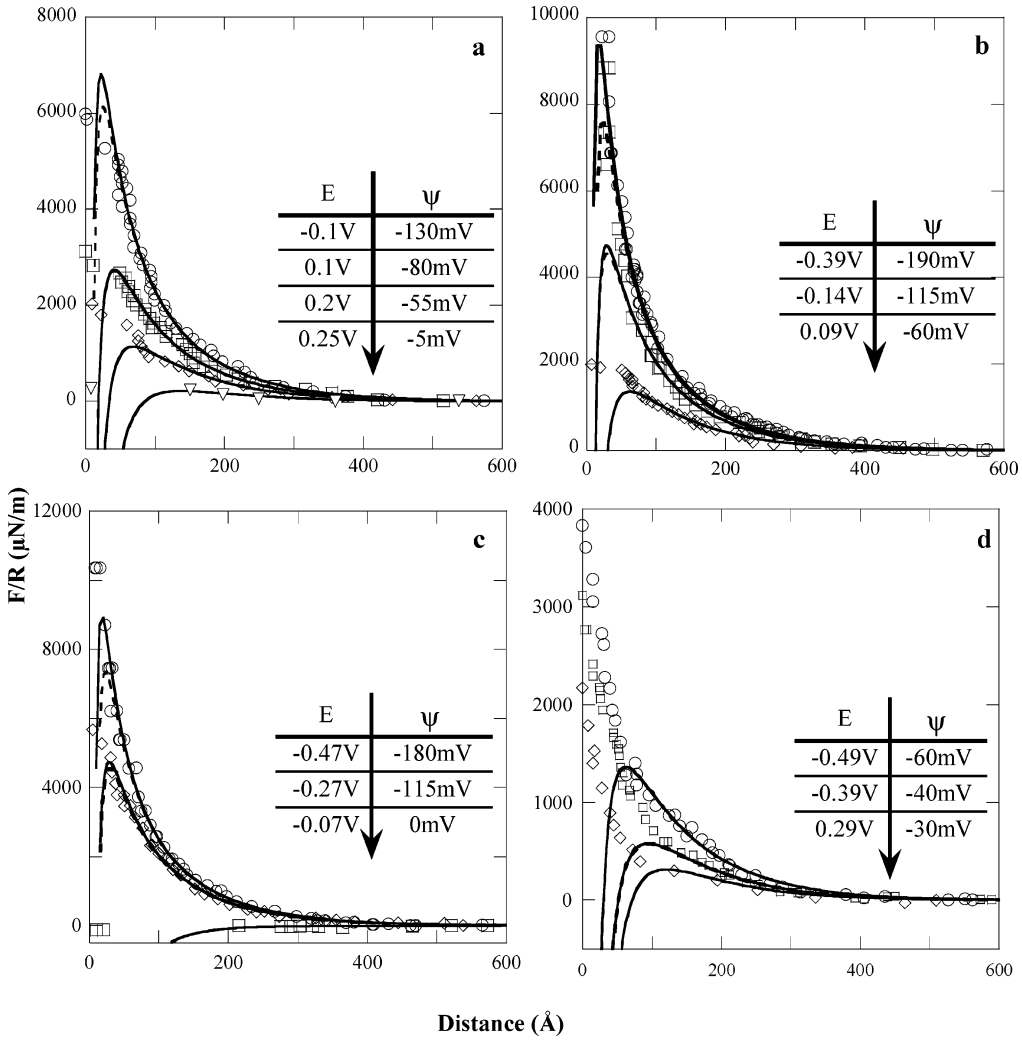

Figure 2. Measured and theoretical forces (normalized by the radius of curvature) between a gold electrode in a mica surface for different pyridine concentrations and at different applied potential. The Hamaker constant is 8.4×10^{-20} J, the mica surface potential is $\Psi^{\infty} = -130$ mV. (a) No pyridine; (b) 0.2 mM pyridine; (c) 1 mM pyridine; (d) 100 mM pyridine.

ously used to explain the forces measured between silica and gold in citrate solution.[11] When pyridine was added to that solution, the long-range double-layer forces disappeared. In contrast to our system, that gold surface was without external potential control, and its charge was caused by citrate adsorption.

A significant change in long-range double-layer forces arising from the presence of pyridine is a shift in the PZF, as determined using the approach of Hillier et al.[34] We define the PZF as the potential for which no forces are measured. More explicitly, we take the value of the measured force at a large separation to avoid the onset of van der Waals forces and to get only a small compression of the interacting double layers (in a 1 mM salt solution, we choose a separation of 300 Å). Minimizing the double-layer overlap also permits the determined PZF value to correspond to the applied potential for which the gold surface potential is zero (since forces between a charged surface and an uncharged wall will be measurable when the double layer of the charged surface is compressed). Previous researchers[34,35] have shown that the PZF is equivalent to the more commonly used PZC, obtained from differential capacitance data. Figure 3 shows the effect of pyridine concentration on the PZF. As the concentration of pyridine increases, the PZF is shifted to more negative values, going from ca. 0.23 V (no pyridine) to ca. −0.1 V (vs Ag/AgCl) for 100 mM pyridine. We suggest that this shift is caused by the replacement of water molecules for pyridine on the gold surface. Pyridine molecules adsorb with

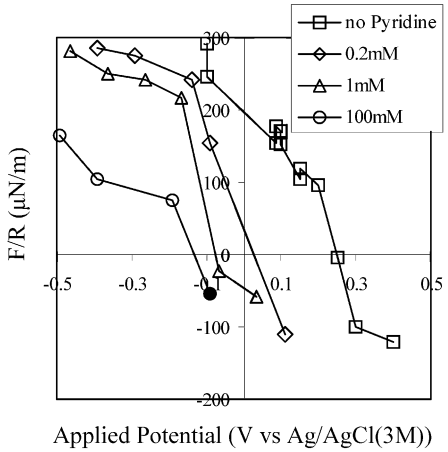

Figure 3. Effect of pyridine on the PZF. The PZF is obtained from the measured forces between gold and mica at different applied potentials for a fixed separation of 300 Å. The PZF is determined as the applied potential at which the measured force is zero. The last point for 100 mM has been extrapolated since the forces were attractive at all separation.

the negative end of the dipole on the gold surface and have a stronger dipole moment than water. The adsorption creates an image charge on the gold surface (i.e., the negative end of the dipole of the pyridine molecule induces a positive charge on

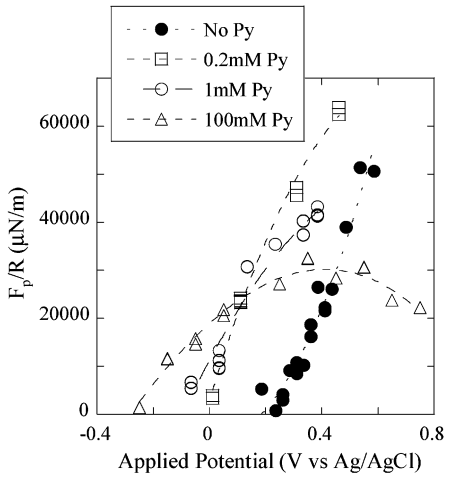

Figure 4. Pull-off forces (normalized by the radius of curvature) as a function of applied potential for solutions of the background salt with different pyridine concentrations added. The lines are to guide the eye.

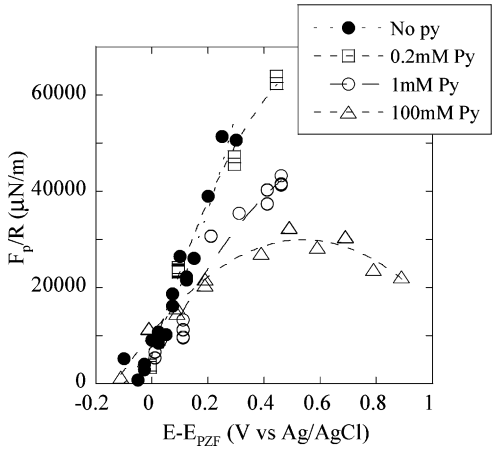

Figure 5. Pull-off forces (normalized by the radius of curvature) as a function of applied potential for different pyridine concentrations. The data are translated by the corresponding PZF. The lines are to guide the eye.

the gold surface) which causes the PZC to move to more negative potentials.[6] The shift in PZF is similar to the shift in PZC observed with polycrystalline gold using chronocoulometry.[6] This shift could explain why high negative surface potentials are not attained for 100 mM pyridine. Figure 2d shows the double-layer forces for the 100 mM pyridine solution. The most repulsive curve obtained has a fitted surface potential of −60 mV, which is less negative than for the other concentrations. In the 100 mM pyridine solution, almost all applied potentials within the double-layer region are more positive than the PZF (due to its shift to more negative values), therefore we cannot apply a potential negative enough to reach the saturation limit without the presence of a faradaic current.

The presence of pyridine also strongly affects adhesion between gold and mica. Figure 4 shows the effect of pyridine concentration on the potential dependence of the pull-off forces. In general, the measured adhesion is stronger at a given potential when pyridine is present. However, no clear trend illustrating how adhesion depends on pyridine concentration is present in the raw data. On the other hand, shown in Figure 5 is the pull-off data with the applied potential translated by the observed PZF. Once the applied potential is expressed as a departure from the PZF, the effect of pyridine adsorption on adhesion shows a systematic behavior with pyridine concentration, demonstrating the importance of the PZF as the key parameter. Increasing the pyridine concentration actually decreases the pull-off forces when the applied potential is shifted by the observed PZF. Clearly, the parameter governing the adhesive strength in this system is the potential away from the PZF rather than the applied potential per se.

As reported in a previous paper,[14] the dependence on applied potential of adhesion between gold and mica can be modeled using a thermodynamic approach based on the definition of the work of adhesion, electrocapillarity, and the Johnson−Kendall−Roberts (JKR) theory of contact mechanics.[36] Briefly, we began with the definition of the work of adhesion

$$W_{ADH} = \gamma_{GL} + \gamma_{ML} - \gamma_{GM} \quad (1)$$

where γ_{GL} is the surface energy of the gold−liquid interface, γ_{ML} is the surface energy of the mica−liquid interface, and γ_{GM} is the surface energy of the gold−mica interface. Thus, the potential dependence of the work of adhesion can be predicted by summing the dependencies on potential of the three surface energy terms. JKR theory is used to relate the work of adhesion to the measured pull-off force.

To obtain a working equation for each of the surface energy terms, we took advantage of the electrocapillary formalism often utilized for the mercury-solution interface, which relates changes in surface potential to the surface charge density (the so-called Lippmann equation)

$$\sigma_{GL} = -\left(\frac{d\gamma_{GL}}{dE}\right)_{P,T,n_i} \quad (2)$$

The potential dependence of γ_{GL} can be obtained directly from electrochemical measurements, or one can use available literature data and integrate eq 2 to obtain γ_{GL}. The mica−liquid surface energy (γ_{ML}) is independent of the applied potential because mica is a good insulator. To allow for a potential dependence of the gold−mica interfacial energy, we need to assume charge separation at the interface. An expression for the potential dependence of γ_{GM} can be developed using eq 2 once the capacitance (C_{GM}) at the interface is estimated.[37] The resulting expression for the gold-mica surface energy is be given by

$$\gamma_{GM} = -C_{GM}(E - E_{PZC}^{GL})^2 - \sigma^0(E - E_{PZC}^{GL}) + \gamma_{GM}^0 \quad (3)$$

with the potential scale expressed as a departure from the gold−liquid PZC (E_{PZC}^{GL}). Here σ^0 and γ_{GM}^0 are the charge density and surface energy, respectively, of the gold−mica interface at the E_{PZC}^{GL}. Combining the potential dependencies of those three surface energies allows the prediction of the work of adhesion, as shown below (eq 4). This relation allows one to predict the potential dependence of the work of adhesion in terms of two physically interpretable model parameters: the work of adhesion at the PZC of the gold−liquid interface ($\Delta\gamma^0 = \gamma_{GL}^0 + \gamma_{ML}^0 - \gamma_{GM}^0$) and the charge density at the gold−mica interface at the PZC of the gold−liquid interface (σ_{GM}^0)

$$W_{ADH} = -\int\int C_{GL}\, dE + (C_{GM}(E - E_{PZC}^{GL})^2 + \sigma_{GM}^0(E - E_{PZC}^{GL})) + (\gamma_{GL}^0 + \gamma_{ML}^0 - \gamma_{GM}^0) \quad (4)$$

Stolberg et al.[6] developed an approach relying on chronocoulometry measurements combined with the use of the Lippmann equation to obtain the relative interfacial energies for polycrystalline gold in solution with different pyridine concentrations. Their analysis was used with polycrystalline and

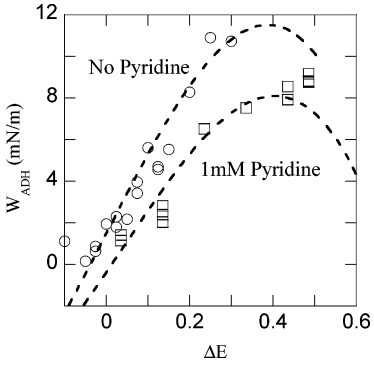

Figure 6. Measured and predicted value of the work of adhesion (W_{ADH}) as a function of applied potential. The measured work of adhesion was obtained from the pull-off measurements using JKR theory, and the applied potential was translated by the PZF. The predicted values were obtained from using the data of Stolberg et al.[6] for the surface energy of the gold−liquid interface and using the following parameters: a capacitance of 50 μF/cm^2, $\sigma^0 = 35$ μC/cm^2, and $\Delta\gamma^0 = 1$ mJ/ m^2 for the no pyridine data; a capacitance of 35 μF/ cm^2, $\sigma^0 = 16$ μC/cm^2, and $\Delta\gamma^0 = 0.5$ mJ/m^2 for the case with 1 mM pyridine.

single-crystal gold surfaces. They were able to obtain the potential dependence of the pyridine surface excess on gold and used this information to develop adsorption isotherms. The surface energy curves obtained by Stolberg et al. follow the typical inverted parabola with a maximum at the PZC. An increase in pyridine concentration has two main effects on the surface energy: a systematic reduction of the surface energy and a shift in the PZC to more negative values. By use of Stolberg's data for the gold−liquid interfacial energy, we were able to use the electrocapillary approach outlined above to predict the effect of pyridine on the adhesion between gold and mica. Shown in Figure 6 is the work of adhesion between the gold electrode and the mica surface for two solutions: for background electrolyte and for 1 mM pyridine added to the background electrolyte. The lines in Figure 6 are best-fit model predictions.

The electrocapillary analysis allows us to gain insight into the behavior of the gold−mica interface as the applied potential is varied. From the Stolberg data, we see that the value of the gold−liquid surface energy goes down by as much as 50% when 1 mM pyridine is added to the background salt solution. On the other hand, the measured adhesion for the background salt only and with 1 mM pyridine added is very similar (see Figure 6). Therefore, to compensate, the gold−mica surface energy necessarily decreases by nearly the same amount as the gold−liquid interfacial energy so as to maintain a similar magnitude in adhesion. Our force measurements thus provide evidence of the coupling of these two surface energies as discussed by Horn et al.[37]

Using the electrocapillary approach to model the adhesion also provides evidence of a change in the capacitance of the gold−mica interface caused by the presence of pyridine. The gold−liquid surface energy curves obtained by Stolberg et al. (which look like a series of inverted parabolas) display a change in curvature with increasing pyridine concentration. When pyridine is present, the surface energy curves open up reflecting a slower drop in the gold−liquid surface energy with increasing potential (past the PZC). This would indicate a general increase in adhesion with increasing pyridine concentration. However, the opposite effect is observed when pyridine is present; the adhesion decreases with increased pyridine (once the data is translated by the PZF, see Figure 5). Thus, the capacitance of the gold−mica interface must also decrease in the presence of pyridine. A smaller value of the gold−mica capacitance may indicate that some pyridine is still trapped at the interface (pyridine is larger and has a lower dielectric constant than water).

Conclusion

In this work, we have shown that small amounts of pyridine in a $KClO_4$ solution have a pronounced impact on surface forces and adhesion between a gold electrode and a mica surface. While presence of pyridine does not have a significant impact on mica−mica forces (except for increasing the non-DLVO repulsive forces slightly), the effect of pyridine on gold−mica interactions is more pronounced. As in the mica−mica interactions, long-range double-layer forces are still present in the presence of pyridine, and large negative surface potentials are observed for all but the highest pyridine concentration. Significantly, however, a large shift in the PZF is measured. We suspect that this shift in PZF is what prevents us from measuring strongly repulsive interactions at the highest pyridine concentration studied (100 mM).

The most dramatic effect of pyridine addition is on the pull-off forces measured. The pyridine-induced shift in the PZF is clearly visible from the potential dependence of the pull-off forces for different pyridine concentrations. Shifting the applied potential by the PZF reveals a systematic effect of pyridine concentration on pull-off forces, showing that the potential translated by the PZF is the relevant governing parameter in this system. An electrocapillary approach developed previously allows us to model the potential-dependent adhesion data and shows new evidence of the coupling of the gold−liquid and gold−mica interfacial energies. The reduction of the gold−liquid interfacial energy due to pyridine reduces the gold−mica energy by the same amount, highlighting the relationship between these two components. Finally, we also see evidence of a change in the capacitance of the gold−mica interface, suggesting that pyridine is trapped at this interface.

Acknowledgment. This work was funded through National Science Foundation via the Materials Research Science and Engineering program grant DMR 0213706 and also by NSF Grant CTS-9907687.

References and Notes

(1) Moffat, T. P. *J. Phys. Chem. B* **1998**, *102*, 10020.
(2) Matsuoka, M.; Murai, J.; Iwakura, C. *J. Electrochem. Soc.* **1992**, *139*, 2466.
(3) Zamborini, F. P.; Cambell, J. K.; Crooks, R. M. *Langmuir* **1998**, *14*, 640.
(4) Lipkowski, J.; Stolberg, L.; Yang, D.-F.; Pettinger, B.; Mirwald, S.; Henglein, F.; Kolb, D. M. *Electrochim. Acta* **1994**, *39*, 1045.
(5) Lipkowski, J.; Stolberg, L. Molecular adsorption at gold and silver electrodes. In *Adsorption of Molecules at Metal Electrodes*; Lipkowski, J. R., Philip, N.; Eds.; VCH Publishing: New York, 1992; p 414.
(6) Stolberg, L.; Richer, J.; Lipkowski, J.; Irish, D. E. *J. Electroanal. Chem.* **1986**, *207*, 213.
(7) Hamelin, A.; Morin, S.; Richer, J.; Lipkowski, J. *J. Electroanal. Chem.* **1989**, *272*, 241.
(8) Sung, Y. E.; Thomas, A.; Gamboaaldeco, M.; Franaszczuk, K.; Wieckowski, A. *J. Electroanal. Chem.* **1994**, *378*, 131.
(9) Nanbu, N.; Kitamura, F.; Ohsaka, T.; Tokuda, K. *J. Electroanal. Chem.* **1999**, *470*, 136.
(10) Rosslee, C.; Abbott, N. L. *Curr. Opin. Colloid Interface Sci.* **2000**, *5*, 81.
(11) Larson, I.; Chan, D. Y. C.; Drummond, C. J.; Griesier, F. *Langmuir* **1997**, *13*, 2429.
(12) Bockris, J. O. M.; Reddy, A. K. N. *Modern Electrochemistry*; Plenum Press: New York, 1970; Vol. 2.
(13) Frechette, J.; Vanderlick, T. K. *Langmuir* **2001**, *17*, 7620.
(14) Frechette, J.; Vanderlick, T. K. *Langmuir* **2005**, *21*, 985.

(15) Tabor, D.; Winterton, R. H. S. *Proc. R. Soc. London, Ser. A* **1969**, *312*, 435.
(16) Israelachvili, J. N.; Adams, G. E. *J. Chem. Soc., Faraday Trans. 1* **1978**, *74*, 975.
(17) Knarr, R. The interaction of surfaces across rough, metal-containing intefaces. Ph.D., University of Pennsylvania, Philadelphia, 1999.
(18) Ives, D. J. G.; Janz, G. J. *Reference electrodes, theory and practice*; Academic Press: New York, 1961.
(19) Israelachvili, J. N. *J. Colloid Interface Sci.* **1973**, *44*, 259.
(20) Clarkson, M. T. *J. Phys. D: Appl. Phys.* **1989**, *22*, 475.
(21) Levins, J. M.; Vanderlick, T. K. *Langmuir* **1994**, *10*, 2389.
(22) Levins, J. M.; Vanderlick, T. K. *J. Colloid Interface Sci.* **1993**, *158*, 223.
(23) Knarr, R.; Quon, R. A.; Vanderlick, T. K. *Langmuir* **1998**, *14*, 6414.
(24) Levins, J. M.; Vanderlick, T. K. *J. Colloid Interface Sci.* **1997**, *185*, 449.
(25) Clavilier, J.; Nguyen Van Huong, C. *J. Electroanal. Chem.* **1977**, *80*, 101.
(26) Derjaguin, B. V.; Landau, L. *Acta Physicochim. U.R.S.S.* **1941**, *14*, 633.
(27) Verway, E. J. W.; Overbeek, J. T. *Theory of Stability of Lyophobic Colloids*; Elsevier: New York, 1948.
(28) Gomez, M. M.; Garcia, M. P.; San Fabian, J.; Vasquez, L.; Salvarezza, R. C.; Arvia, A. J. *Langmuir* **1997**, *13*, 1317.
(29) Pashley, R. M.; Israelachvili, J. N. *J. Colloid Interface Sci.* **1984**, *101*, 511.
(30) Yoon, R.-H.; Vivek, S. *J. Colloid Interface Sci.* **1998**, *204*, 179.
(31) Pashley, R. M. *J. Colloid Interface Sci.* **1981**, *83*, 531.
(32) Berhouet, S.; Toulhoat, H. *Langmuir* **1994**, *10*, 1832.
(33) Shubin, V. E.; Kekicheff, P. *J. Colloid Interface Sci.* **1993**, *155*, 108.
(34) Hillier, A. C.; Kim, S.; Bard, A. J. *J. Phys. Chem.* **1996**, *100*, 18808.
(35) Wang, J.; Bard, A. J. *J. Phys. Chem. B* **2001**, *105*, 5217. *Electroanal. Chem.* **1981**, *125*, 177.
(36) Johnson, K. L.; Kendall, K.; Roberts, A. D. *Proc. R. Soc. London, Ser. A* **1971**, *324*, 301.
(37) Antelmi, D. A.; Connor, J. N.; Horn, R. G. *J. Chem. Phys. B* **2004**, *108*, 1030.